## ORIGINAL RESEARCH

# Chromosome 10q24.32 Variants Associate With Brain Arterial Diameters in Diverse Populations: A Genome-Wide Association Study

Minghua Liu ⓘ, PhD; Farid Khasiyev ⓘ, MD; Sanjeev Sariya ⓘ, MS; Antonio Spagnolo-Allende ⓘ, MD, MPH; Danurys L Sanchez ⓘ, BA; Howard Andrews, PhD; Qiong Yang ⓘ, PhD; Alexa Beiser ⓘ, PhD; Ye Qiao ⓘ, PhD; Emy A Thomas ⓘ, MS; Jose Rafael Romero ⓘ, MD; Tatjana Rundek ⓘ, MD, PhD; Adam M Brickman ⓘ, PhD; Jennifer J Manly ⓘ, PhD; Mitchell SV Elkind ⓘ, MD, MS; Sudha Seshadri ⓘ, MD; Christopher Chen ⓘ, MD; Saima Hilal ⓘ, MD, PhD; Bruce A Wasserman ⓘ, MD; Giuseppe Tosto ⓘ, MD PhD; Myriam Fornage ⓘ, PhD; Jose Gutierrez ⓘ, MD, MPH

**BACKGROUND:** Brain arterial diameters (BADs) are novel imaging biomarkers of cerebrovascular disease, cognitive decline, and dementia. Traditional vascular risk factors have been associated with BADs, but whether there may be genetic determinants of BADs is unknown.

**METHODS AND RESULTS:** The authors studied 4150 participants from 6 geographically diverse population-based cohorts (40% European, 14% African, 22% Hispanic, 24% Asian ancestries). Brain arterial diameters for 13 segments were measured and averaged to obtain a global measure of BADs as well as the posterior and anterior circulations. A genome-wide association study revealed 14 variants at one locus associated with global BAD at genome-wide significance ($P<5\times10^{-8}$) (top single-nucleotide polymorphism, rs7921574; $\beta=0.06$ [$P=1.54\times10^{-8}$]). This locus mapped to an intron of *CNNM2*. A trans-ancestry genome-wide association study meta-analysis identified 2 more loci at *NT5C2* (rs10748839; $P=2.54\times10^{-8}$) and *AS3MT* (rs10786721; $P=4.97\times10^{-8}$), associated with global BAD. In addition, 2 single-nucleotide polymorphisms colocalized with expression of *CNNM2* (rs7897654; $\beta=0.12$ [$P=6.17\times10^{-7}$]) and *AL356608.1* (rs10786719; $\beta=-0.17$ [$P=6.60\times10^{-6}$]) in brain tissue. For the posterior BAD, 2 variants at one locus mapped to an intron of *TCF25* were identified (top single-nucleotide polymorphism, rs35994878; $\beta=0.11$ [$P=2.94\times10^{-8}$]). For the anterior BAD, one locus at *ADAP1* was identified in trans-ancestry genome-wide association analysis (rs34217249; $P=3.11\times10^{-8}$).

**CONCLUSIONS:** The current study reveals 3 novel risk loci (*CNNM2*, *NT5C2*, and *AS3MT*) associated with BADs. These findings may help elucidate the mechanism by which BADs may influence cerebrovascular health.

**Key Words:** chromosome 10q24.32 ■ *CNNM2* ■ genome-wide association studies ■ larger brain arterial diameters

Dolichoectasia has been defined by elongated and tortuous arteries[1] and it is usually associated with smoking, male sex, and aging.[2] The diagnosis of dolichoectasia has been historically ascertained by visual inspection of neuroimaging or, more recently, using a fixed arterial diameter cutoff for the basilar

---

## CLINIC PERSPECTIVE

### What Is New?
- We identified 3 novel risk loci (*CNNM2*, *NT5C2*, and *AS3MT*) associated with brain arterial diameters in trans-ancestry genome-wide association analysis.

### What Are the Clinical Implications?
- These findings may help elucidate the mechanism by which brain arterial diameters may influence cerebrovascular health.

### Nonstandard Abbreviations and Acronyms

| | |
|---|---|
| **ARIC** | Atherosclerosis Risk in Communities |
| **BAD** | brain arterial diameter |
| **BORC** | BLOC-one-related complex |
| **CADD** | Combined Annotation Dependent Depletion |
| **EDIS** | Epidemiology of Dementia in Singapore |
| **eQTL** | expression quantitative trait loci |
| **FHS** | Framingham Heart Study |
| **FUMA** | Functional Mapping and Annotation |
| **GTEx** | Genotype-Tissue Expression |
| **MAGMA** | Multi-Marker Analysis of GenoMic Annotation |
| **MCS** | Memory Clinic in Singapore |
| **MR** | Mendelian randomization |
| **MR-MEGA** | Meta-Regression of Multi-Ethnic Genetic Association |
| **MsigDB** | Molecular Signatures Database |
| **MTAG** | Multi-Trait Analysis of GWAS |
| **NOMAS** | The Northern Manhattan Study |
| **SEED** | Singapore Epidemiology of Eye Diseases |
| **WHICAP** | Washington Heights–Inwood Columbia Aging Project |

artery.[3] Although these methods are easy to use, they simplify the biological meaning of the continuum of intracranial arterial diameters in brain health and neglect arterial-size expectations based on age, sex, and head size.[4] A previous study validated the principle that arterial diameters measured continuously and adjusted for head size relate to health outcomes in a nonlinear fashion, indicating that people with very small or very large arterial diameters are at a higher risk of vascular events.[5] Furthermore, dilated brain arterial diameters (BADs) are associated with a higher risk of dementia[6] and steeper cognitive decline.[7] Smaller arterial diameters causing stenosis, usually related to atherosclerosis, are intuitively related to adverse health outcomes,[8,9] but less is known about the underlying nature of dilated brain arteries.

Larger arterial diameters have been described in people with connective tissue disorders such as Marfan syndrome,[10] Ehlers-Danlos,[11] and Arterial Tortuosity Syndrome,[12] among others. These monogenic diseases are usually rare and detected in younger patients. Furthermore, there is a clear association between larger arterial diameters and vascular risk factors, especially hypertension.[4,13] Although hypertension is highly prevalent in elderly populations, the heterogeneity of brain arterial phenotypes in people with vascular risk factors suggests that a specific genetic profile might partially be responsible for higher risk of brain arterial dilatation. Therefore, we hypothesize that in the general population, there may exist less pathogenic but more prevalent genetic variants that are associated with BADs. Identifying such a genetic profile may shed light into possible mechanistic links between large BADs and the observed brain outcomes. To test our hypothesis, we leveraged diverse population cohorts within and outside the United States to investigate associations between BADs and Alzheimer disease (AD), stroke, and white matter hyperintensities volume.

## METHODS

Studies participating in this meta-analysis have separate and specific data request and approval policies, depending on local, national, and international laws and regulations. Because of restrictions based on such privacy laws and regulations and informed consent of the participants, data cannot be made freely available in a public repository for any of the participating studies. Requests for information on procedures and formal data requests can be submitted to investigators from the individual studies or to the corresponding author for referral.

### Sampled Populations
#### Atherosclerosis Risk in Communities Study

The ARIC (Atherosclerosis Risk in Communities) study is a population-based prospective cohort study of vascular risks and includes 15 792 persons aged 45 to 64 years at baseline (1987 to 1989) randomly chosen from 4 US communities.[14] Cohort members completed 7 clinic examinations, conducted between 1987 and 2019. Dementia and dementia subtypes were adjudicated beginning in 2011 using in-person interviews and cognitive testing, chart reviews, and telephone

surveys.[15] Written informed consent was provided by all study participants, and the study design and methods were approved by institutional review boards at the collaborating medical institutions (The Johns Hopkins University, Wake Forest University, the University of Mississippi Medical Center, and the University of Minnesota).

### The Northern Manhattan Study

The NOMAS (Northern Manhattan Study) is an ongoing prospective cohort initially focused on determining the incidence of stroke and vascular events in a diverse urban population. Participants were recruited using random digit dialing between 1993 and 2001 with the following eligibility criteria: (1) age 40 years or older, (2) clinically stroke-free, and (3) resident of Northern Manhattan for at least 3 months. In-person cognitive testing has been performed 3 times since 2011 in surviving participants. Dementia was adjudicated by consensus between a neurologist and a neuropsychologist.

The institutional review boards at Columbia University Medical Center and the University of Miami approved the study. All participants provided written informed consent.

### Washington Heights–Inwood Columbia Aging Project Study

The WHICAP (Washington Heights–Inwood Columbia Aging Project) study is a prospective, population-based study of aging and dementia. Established through several recruitment waves, participants were first recruited in 1992 from a random sample of Medicare-eligible adults (aged ≥65 years) residing in the neighborhoods of Washington Heights and Inwood in northern Manhattan. Participants are evaluated longitudinally every 18 to 24 months, with a comprehensive neuropsychological battery, medical and neurologic examination, and survey about health-related outcomes.[16] Dementia and dementia subtypes are adjudicated in a consensus conference that includes neurologists and neuropsychologists. The institutional review boards at Columbia University Medical Center approved the study. All participants provided written informed consent.

### Epidemiology of Dementia in Singapore Study

The EDIS (Epidemiology of Dementia in Singapore) study was a population-based cohort study conducted in southwestern Singapore between 2004 and 2011. It recruited participants who participated in the baseline visit of the SEED (Singapore Epidemiology of Eye Diseases) study, which comprised 10 033 adults of Chinese, Malay, and Indian ancestry, aged 40 to 80 years.[17–20] Briefly, the EDIS study consisted of 3 independent

population cohorts with a common protocol. In all studies, individuals aged 40 to 80 years were selected by an age-stratified random sampling method from a computer-generated random list of names provided by the Ministry of Home Affairs. The study was approved by the institutional review board of Singapore Eye Research Institute. Written informed consent was obtained, in the preferred language of participants, by bilingual study coordinators prior to recruitment into the study.

### Memory Clinic in Singapore Study

The MCS (Memory Clinic in Singapore) study included patients attending the National University Hospital and St Luke's Hospital memory clinics between 2009 and 2015. Patients were referred by primary care as well as secondary and tertiary care facilities because of consistent memory complaints and were assessed by a team of clinicians, psychologists, and nurses in the Memory Aging and Cognition Center, National University of Singapore. The institutional review boards at National University Hospital approved the study. All participants provided written informed consent.

### Framingham Heart Study

The FHS (Framingham Heart Study) started enrolling community-based participants in 1949. In 1971, all descendants of the original cohort (ie, offspring cohort, requiring at least 1 parent from the original cohort) and their spouses were invited to participate in a follow-up study, and, since then, they have been followed prospectively. The initial cohort consisted of 5124 men and women; 88% of survivors (3539 of 4031) participated in examination 7 in 1998 to 2001. Participants who survived the seventh examination were invited to undergo brain magnetic resonance imaging (1999 to 2005), with a final sample of 2144 stroke-free, community-based participants. For these analyses, we used an FHS subsample with available magnetic resonance angiography (MRA) as part of the stroke case study. The institutional review boards at Boston Medical Center approved the study. All participants provided written informed consent.

We followed the Strengthening the Reporting of Observational Studies in Epidemiology reporting guidelines for cohort studies.[21]

## Measurement of Bad

Brain MRA acquisition parameters by cohort are reported in Table S1. BADs and brain arterial lengths were obtained from all available MRA images using commercial software (LKEB Automated Vessel Analysis [LAVA], Leiden University Medical Center, The Netherlands, build date October 19, 2018). Briefly, this software uses a flexible 3-dimensional D tubular

nonuniform rational B-splines model to automatically identify the margins of the arterial lumen based on voxel intensity[22,23] with excellent reliability (Figure 1).[23] The 13 arterial segments measured included the bilateral intracranial internal carotid artery, middle cerebral artery, anterior cerebral artery, posterior cerebral artery, vertebral artery, and posterior communicating arteries, plus the basilar artery. The location of measurement was aimed at the largest portion of a given segment free of focal stenosis, with good to excellent reliability.[24] For arteries visualized in the axial source MRA images but not large enough to be reconstructed, we systematically assigned the smallest measured diameters for the artery in the sample minus 10%. We counted arteries not visualized on axial source MRA images to create a score of absent arteries. We transformed each artery diameter distribution into normal scores and obtained the global (all 13 arteries), anterior (internal carotid arterial, middle cerebral arterial, anterior cerebral arterial, and posterior communicating if available), and posterior (vertebral arterial, basilar arterial, and posterior cerebral arterial if available) arterial diameter scores by cohort as the principal dependent variable.

## Genotyping and Imputation

A detailed description of genotyping, quality control, and imputation in each study is provided in Table S2.[25–27] All analyses were conducted on autosomal chromosomes. Genotypes with a missing rate >10%, significant Hardy–Weinberg equilibrium $P$ value ($P<5\times10^{-8}$), or poor imputation quality ($r^2<0.3$) were excluded from the analyses.

## Genome-Wide Association Analysis

In each study and self-reported racial/ancestry strata, linear regression models were used to test the association between genetic variants and BAD (global, anterior, and posterior scores) using an additive genetic model, adjusted for sex, age, head size, number of absent arteries, and population-specific principal components of ancestry. Genome-wide association study (GWAS) results were subjected to quality control analyses using EasyQC (https://www.uni-regensburg.de/medizin/epidemiologie-praeventivmedizin/genetische-epidemiologie/software/) and combined by meta-analysis by METAL[28] (https://csg.sph.umich.edu/abecasis/Metal/) using a fixed-effect inverse variance–based method for variants included in at least 2 studies. Variants with minor allele frequencies <1% were excluded after the meta-analyses. A trans-ancestry meta-analysis of GWAS was conducted to account for heterogeneity in allelic effect that is correlated with ancestry by Meta-Regression of Multi-Ethnic Genetic Association (MR-MEGA) (https://genomics.ut.ee/en/tools).[29] Ancestry-specific meta-analyses
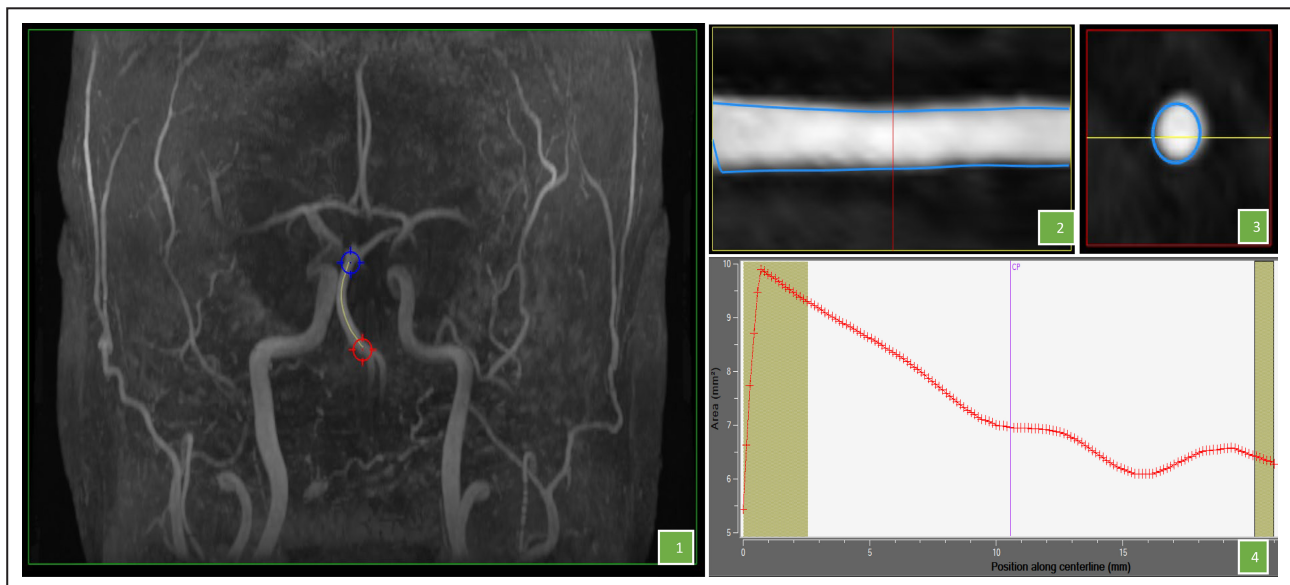


**Figure 1.  LKEB LAVA.**
This software measures the arterial diameters several times across a segment via multiplanar reformatted imaging. This creates cross-sectional views of the blood vessels at any orientation and at any point along the vessel's centerline. Step 1: the user selects a segment of the blood vessel to analyze. Step 2: magnetic resonance angiography (MRA) image data for the selected segment is reformatted into a 3-dimensional volume, with the centerline of the vessel as the axis of rotation. Step 3: the user can then create cross-sectional views of the vessel at any point along the centerline using the MPR tool. Step 4: the arterial diameter is measured on each cross-sectional view, providing multiple measurements of the diameter across the selected segment. The measured diameters are then used to calculate average, maximum, and minimum diameters, as well as diameter variations along the segment.

were also performed to identify ancestry-specific variants. Multi-Trait Analysis of GWAS (MTAG, https://ctg.cncr.nl/software/magma) tool[30] was used for multivariate analysis of anterior and posterior BAD to boost the statistical power to detect genetic associations. Adjustment for winner's curse was performed to provide bias-reduced estimates by bootstrap re-sampling (BR_squared) method using "winnerscurse" R package (R Foundation for Statistical Computing).[31] An association with $P<5\times10^{-8}$ was considered genome-wide significant, whereas $P<1.0\times10^{-5}$ was used as suggestive evidence for marker associations.

## Gene-Based Association Analysis and Gene-Set Enrichment

We performed a gene-based association analysis based on summary statistics using Multi-Marker Analysis of GenoMic Annotation (MAGMA; version 1.07),[32] implemented by Functional Mapping and Annotation (FUMA).[33] Variants with $P<1\times10^{-5}$ were mapped to the nearest gene within 50 kb or expression quantitative trait loci (eQTL) genes in Genotype-Tissue Expression (GTEx) project data version 8[34] from brain tissues: amygdala, anterior cingulate cortex (BA24), caudate (basal ganglia), cerebellar hemisphere, cerebellum, cortex, frontal cortex (BA9), hippocampus, hypothalamus, nucleus accumbens (basal ganglia), putamen (basal ganglia), spinal cord (cervical c-1), and substantia nigra. Mapped genes were then tested for tissue specificity in 30 general GTEx tissues using the precalculated differentially expressed gene (DEG) sets integrated in the GENE2FUNC of FUMA.[29] Hypergeometric enrichment tests were performed via GENE2FUNC against predefined gene sets obtained from Molecular Signatures Database (MsigDB),[35] WikiPathways,[36] and GWAS catalog.[37] We used a Bonferroni-corrected $P<0.05$ to define statistical significance in gene-based analyses.

## Identification of Genomic Risk Loci and Deleteriousness of Lead Single-Nucleotide Polymorphisms

Variants that had at least suggestive evidence ($P<10^{-5}$) were filtered and LD-clumped at $r^2<0.1$ to identify independent loci using FUMA's SNP2GENE function[33] based on the relevant 1000G reference. To investigate the protein coding consequences of lead independent variants associated with BAD, the Combined Annotation Dependent Depletion (CADD) score was estimated. We used the threshold of 12.37 to determine whether a lead variant was deleterious.[38] When the CADD score of a lead variant was smaller than

12.37, we assessed whether its proxy variants ($r^2>0.8$) were deleterious instead.

## Pleiotropic Association Analysis With Gene Expression

We used SMR software[39] to test for a pleiotropic association between BAD traits and gene expression. We used summary-level data from our GWAS analyses and data on eQTL from the BrainMeta project version 2.[40] There are 5967 cis-eQTLs with eQTL $P<5\times10^{-8}$. We used a Bonferroni-corrected $P<8.4\times10^{-6}$ (0.05/5967) to define statistical significance in pleiotropic association analyses.

## Two-Sample Mendelian Randomization Analysis

We conducted 2-sample Mendelian randomization (MR) analysis using genetic instruments from the present analyses to assess whether BAD is a causal factor for AD, stroke, and white matter hyperintensities volume. The summary statistics for AD, stroke, and white matter hyperintensities volume were used in this analysis.[41–43] To avoid bias driven by correlated instruments, variants with BAD association $P<1.0\times10^{-5}$ were LD-clumped at $r^2<0.01$[44] against the 1000 Genome LD reference calculated for African, European, Asian, and Hispanic populations. Variants with minor allele frequencies <0.01 in the reference population were excluded from MR analysis. Causal association was primarily evaluated using the inverse variance–weighted method. To assess the presence of horizontal pleiotropy (ie, that variants influence the outcome trait via independent pathways other than the exposure trait), we used the simple mode method, weighted mode method, inverse variance–weighted method, median-based method, and MR-Egger method. All MR analyses were performed using TwoSampleMR in R package.[45]

# RESULTS

## Multi-Ancestry GWAS Identifies a Novel Locus Associated With BAD

We conducted a multi-ancestry GWAS for BAD levels in 4150 participants, including 1650 from European, 583 from African, 920 from Hispanic, and 997 from Asian ancestries. The mean age of the participants among the studies ranged from 70 to 76 years, with proportions of women ranging from 52% to 64%. Detailed demographic information is presented in Table 1.

We identified 14 variants at one locus associated with global BAD at genome-wide significance ($P<5\times10^{-8}$) (Figure 2A). This locus mapped to an intron of *CNNM2*. One copy of the C allele (minor allele frequency, 0.42) for the lead single-nucleotide variant

**Table 1.  Demographic Information of Studies**

| Cohort | ARIC | NOMAS | WHICAP | EDIS | MCS | FHS |
|---|---|---|---|---|---|---|
| No. | 1565 | 1092 | 290 | 647 | 350 | 206 |
| Age, mean (SD), y | 75.8 (5.3) | 70.1 (8.4) | 77.2 (6.5) | 70.2 (6.6) | 71.0 (8.2) | 72.7 (11.7) |
| Women, % | 58.8 | 60.5 | 64.1 | 51.7 | 55.7 | 54.3 |
| Self-reported racial and ethnic identity or geographic ancestry, % | | | | | | |
| European/White | 74.3 | 13.8 | 44.8 | - | - | 100.0 |
| African/Black/African American | 25.7 | 16.6 | 55.2 | - | - | - |
| Hispanic | - | 69.6 | - | - | - | - |
| Asian | - | - | - | 100.0 | 100.0 | - |
| Hypertension, % | 74.9 | 68.1 | 63.1 | 80.8 | 67.8 | 68.4 |
| Diabetes, % | 33.9 | 19.0 | 20.2 | 37.3 | 31.8 | 23.9 |
| Dyslipidemia, % | 56.0 | 45.0 | 33.9 | 76.0 | 71.4 | 51.6 |
| Smoking, % | 6.0 | 52.7 | 5.2 | 27.9 | 7.1 | 9.3 |

ARIC indicates Atherosclerosis Risk in Communities; EIDS, Epidemiology of Dementia In Singapore; FHS, Framingham Heart Study; MCS, Memory Clinic in Singapore; NOMAS, The Northern Manhattan Study; and WHICAP, Washington Heights-Inwood Community Aging Project.

(SNV) rs7921574 was associated with 6% increased global BAD ($P=1.54\times10^{-8}$) (Table 2; Figure S1A and S1B). We also identified 2 intronic variants in *TCF25* associated with posterior BAD at genome-wide significance (Figure 2B). One copy of the C allele (minor allele frequency, 0.29) for the lead SNV rs35994878 was associated with 11% increased posterior BAD ($P=2.94\times10^{-8}$) (Table 2; Figure S1C and S1D; Table S3). We did not observe any genome-wide significant association for anterior BAD (Figure 2C). No genomic inflation was observed for any of the BAD analyses (Figure S2). The genomic inflation factor (lambda) was 1.01, 1.02, and 1 for global, anterior, and posterior BAD, respectively. We also performed ancestry-specific regional Manhattan plots for top SNVs in global (rs7921574), anterior (rs7921574), and posterior (rs35994878) diameter meta-analysis, respectively (Figures S3 through S5), but did not observe ancestry-specific genome-wide significant associations.

In the trans-ancestry genome-wide association analysis for global BAD, in addition to SNVs in *CNNM2*, we identified one genome-wide significant SNV near *NT5C2* (rs10748839; $P=2.54\times10^{-8}$) and one in *AS3MT* (rs10786721; $P=4.97\times10^{-8}$). All were located within 10q24.32. For anterior BAD, we identified one locus at *ADAP1* (rs34217249; $P=3.11\times10^{-8}$) (Table 3). In the Hispanic-specific analysis, we identified a genome-wide significant locus at *LOC107986223* for global BAD; three loci at *TGFBR2*, *LOC105374506*, and *LOC105376292* for posterior BAD (Table S4). We did not observe a genome-wide significant association in European, African, or Asian ancestries (Tables S5 through S7) for global, anterior, or posterior BAD. No genomic inflation was observed in trans-ancestry analysis (Figures S6 through S8).

## Variant Effects Predictions on Protein Coding Sequence

We investigated the predicted deleterious effects of BAD-associated loci using CADD scores. The SNVs and their proxies with CADD scores are shown in Tables 2 and 3. We did not observe a significant CADD score among the genome-wide significant loci associated with BAD. An SNV associated with posterior BAD in the *RAD52* region (rs140934041) showed a significant CADD score (13.45) in Hispanic-specific analysis (Table S4). In addition, SNVs associated with anterior BAD in the *RAPGEF4* and posterior BAD in the *PODXL* region showed significant CADD scores (rs2290378, 16.31; rs888608, 16.63) in Asian-specific analysis (Table S6).

## Gene-Based Association Test and Gene-Set Enrichment

The MAGMA gene-based association analysis identified one locus associated with global BAD ($P<1.50\times10^{-5}$) (Table S8). The significant associations for global BAD included the GWAS located at *AS3MT, CNNM2, NT5C2, ARL3, TMEM180, C10orf32*, and *C10orf32-ASMT*. Genes mapped to GWAS associations with $P<1\times10^{-5}$ were further investigated for gene-set enrichment (Table S9). Three genome-wide significant loci for global BAD, *AS3MT, CNNM2,* and *NT5C2*, were enriched in the white matter lesion progression gene set from the GWAS catalog database (adjusted $P=7.60\times10^{-7}$).

## Tissue-Specific Colocalization Analyses

We performed colocalization analysis for the locus identified in the GWAS and MTAG analysis with
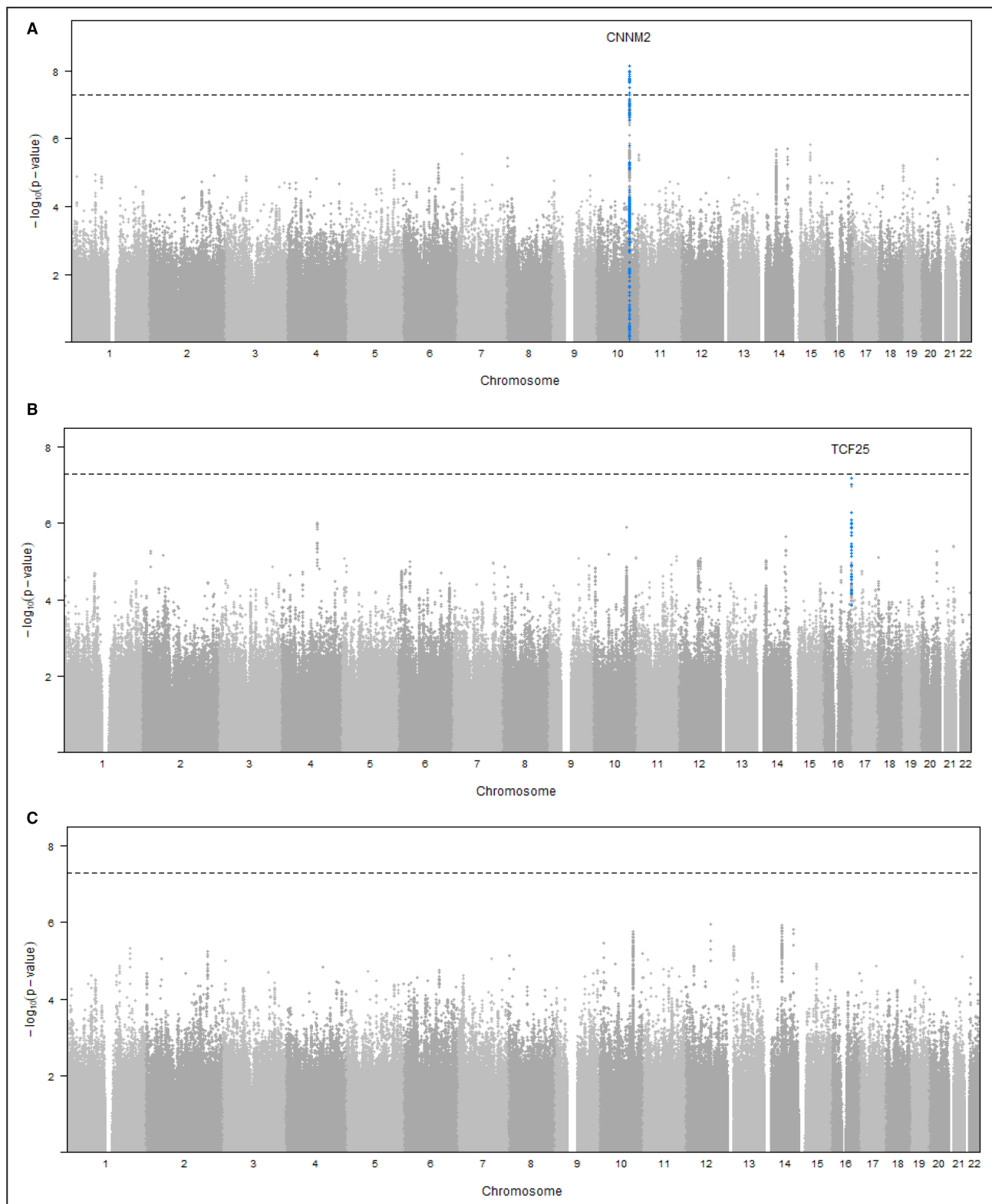
**Figure 2. Genome-wide associations in brain arterial diameter (BAD).**
Manhattan plots for (BAD) show combined genome-wide associations from 6 population-based studies. **A**, Global BAD. **B**, Anterior BAD. **C**, Posterior BAD.

**Table 2.  Variants ($P<5\times10^{-8}$) Associated With BAD**

| SNV | Chromosome | Position (hg 19) | Nearest gene | Relation to gene | Allele1 | Allele2 | AF | beta | SE | beta_BR_ss | P value | CADD |
|---|---|---|---|---|---|---|---|---|---|---|---|---|
| Global | | | | | | | | | | | | |
| rs7921574 | 10 | 104840970 | *CNNM2* | ncRNA_intronic | C | T | 0.42 | 0.06 | 0.01 | 0.03 | 1.54E-08 | 0.33 |
| rs943035 | 10 | 104839152 | *CNNM2* | ncRNA_intronic | C | T | 0.42 | 0.06 | 0.01 | 0.03 | 1.57E-08 | 0.71 |
| rs10883826* | 10 | 104830819 | *CNNM2* | ncRNA_intronic | G | A | 0.42 | 0.06 | 0.01 | 0.03 | 1.58E-08 | 2.25 |
| rs943036 | 10 | 104836047 | *CNNM2* | ncRNA_intronic | C | T | 0.42 | 0.06 | 0.01 | 0.03 | 1.66E-08 | 5.85 |
| rs10883824 | 10 | 104812897 | *CNNM2* | ncRNA_intronic | G | A | 0.42 | 0.06 | 0.01 | 0.03 | 2.12E-08 | 2.98 |
| rs8139 | 10 | 104848123 | *CNNM2* | ncRNA_intronic | A | G | 0.42 | 0.06 | 0.01 | 0.03 | 2.31E-08 | 7.82 |
| rs3740387 | 10 | 104849468 | *CNNM2* | ncRNA_intronic | A | G | 0.42 | 0.06 | 0.01 | 0.03 | 2.33E-08 | 8.71 |
| rs10883817 | 10 | 104755431 | *CNNM2* | ncRNA_intronic | A | G | 0.42 | 0.06 | 0.01 | 0.03 | 2.82E-08 | 0.37 |
| rs3902934 | 10 | 104746649 | *CNNM2* | ncRNA_intronic | G | A | 0.42 | 0.06 | 0.01 | 0.03 | 2.84E-08 | 1.24 |
| rs10883823 | 10 | 104812331 | *CNNM2* | ncRNA_intronic | C | T | 0.42 | 0.06 | 0.01 | 0.03 | 3.35E-08 | 0.25 |
| rs7911789 | 10 | 104756374 | *CNNM2* | ncRNA_intronic | C | T | 0.42 | 0.06 | 0.01 | 0.03 | 3.84E-08 | 0.58 |
| rs67908413 | 10 | 104764989 | *CNNM2* | ncRNA_intronic | C | T | 0.42 | 0.06 | 0.01 | 0.03 | 3.84E-08 | 6.84 |
| rs1890184 | 10 | 104748459 | *CNNM2* | ncRNA_intronic | C | A | 0.42 | 0.06 | 0.01 | 0.03 | 4.26E-08 | 0.62 |
| rs10786733 | 10 | 104794947 | *CNNM2* | ncRNA_intronic | A | G | 0.42 | 0.06 | 0.01 | 0.03 | 4.84E-08 | 4.21 |
| Posterior | | | | | | | | | | | | |
| rs35994878 | 16 | 89949033 | *TCF25* | Intronic | C | T | 0.29 | 0.11 | 0.02 | 0.04 | 2.94E-08 | 1.06 |
| rs8061025 | 16 | 89948397 | *TCF25* | Intronic | A | G | 0.29 | 0.11 | 0.02 | 0.03 | 4.49E-08 | 0.42 |

*Independent variant associated with brain arterial diameter (BAD). Nearest gene with a functional protein or RNA product that either overlaps with the variant or for intergenic variants, the nearest genes upstream and downstream, respectively. The statistics are based on effect allele (Allele1; allele2 is another allele). AF indicates allele 1 frequency; beta_BR_ss, effect size estimate correcting for the winner's curse by bootstrap resampling (BR_squared) method; CADD, combined annotation dependent depletion score; and SNV, single-nucleotide variant.

gene expression using GTEx version 8 eQTL data (Table S10). We identified SNVs associated with *AS3MT* and *C10orf32* expression and global BAD in all 13 brain tissues. We also identified SNVs at TMEM180 in caudate basal ganglia, cerebellar hemisphere, nucleus accumbent basal ganglia, putamen basal ganglia, and spinal cord cervical c-1; SNVs at *CNNM2* in caudate basal ganglia tissues; and SNVs at *NT5C2* and *ARL3* in cerebellum tissue, which colocalized with global BAD. We also performed a transcriptome-wide association analysis for the loci identified in the GWAS with gene expression using BrainMeta project data in global, anterior, and posterior BAD (Table 4). At the transcriptome-wide significance level ($P<8.4\times10^{-6}$), we identified SNVs associated with CNNM2 ($P=6.17\times10^{-7}$) and *AL356608.1* ($P=6.6\times10^{-6}$) expression in global BAD (Figure 3A). We did not observe a transcriptome-wide significant association in anterior or posterior BAD (Figure 3B and 3C).

**Table 3.  Trans-Ancestry Genome-Wide Significant Associations**

| SNV | Chromosome | Position (hg 19) | Nearest gene | Relation to gene | Allele1 | Allele2 | AF | P value | P_Het ANCS | P_Res Het | CADD |
|---|---|---|---|---|---|---|---|---|---|---|---|
| Global | | | | | | | | | | | |
| rs10883805 | 10 | 104708251 | *CNNM2* | ncRNA_intronic | C | T | 0.43 | 1.88E-08 | 0.003 | 0.333 | 4.39 |
| rs10748839 | 10 | 104953547 | *NT5C2* | upstream | C | T | 0.42 | 2.54E-08 | 0.001 | 0.526 | 3.34 |
| rs3902934 | 10 | 104746649 | *CNNM2* | ncRNA_intronic | G | A | 0.42 | 4.55E-08 | 0.026 | 0.329 | 1.24 |
| rs10883814 | 10 | 104737404 | *CNNM2* | ncRNA_intronic | C | T | 0.43 | 4.79E-08 | 0.004 | 0.324 | 3.01 |
| rs12569617 | 10 | 104729996 | *CNNM2* | ncRNA_intronic | C | T | 0.43 | 4.85E-08 | 0.004 | 0.323 | 2.87 |
| rs10786721 | 10 | 104654383 | *AS3MT* | ncRNA_intronic | A | C | 0.43 | 4.97E-08 | 0.004 | 0.384 | 4.52 |
| Anterior | | | | | | | | | | | |
| rs34217249 | 7 | 960642 | *ADAP1* | Intronic | A | G | 0.20 | 3.11E-08 | 2.03E-08 | 0.36 | 2.26 |

Nearest gene with a functional protein or RNA product that either overlaps with the variant or for intergenic variants, the nearest genes upstream and downstream, respectively. The statistics are based on effect allele (Allele1; allele2 is another allele). AF indicates allele 1 frequency; CADD, combined annotation dependent depletion score; P_Het ANCS *P* value for heterogeneity correlated with ancestry; P_Res Het, residual heterogeneity; and SNV, single-nucleotide variant.

**Table 4. Top 10 Colocalization of BAD GWAS and eQTL Associations**

| Probe ID | Probe chromosome | Gene | Probe_bp | SNV | SNV chromosome | SNV bp | Allele1 | Allele2 | AF | beta | SE | beta_BR_ss | P value |
|---|---|---|---|---|---|---|---|---|---|---|---|---|---|
| **Global** | | | | | | | | | | | | | |
| ENSG00000148842.18 | 10 | CNNM2 | 104764015 | rs7897654 | 10 | 104662458 | C | T | 0.28 | 0.12 | 0.02 | 0.06 | 6.17E-07* |
| ENSG00000272912.1 | 10 | AL356608.1 | 104674752 | rs10786719 | 10 | 104637992 | G | A | 0.41 | −0.17 | 0.04 | −0.10 | 6.60E-06* |
| ENSG00000137760.15 | 11 | ALKBH8 | 107404960 | rs2037827 | 11 | 107408592 | C | T | 0.21 | −0.11 | 0.03 | −0.07 | 3.22E-04 |
| ENSG00000186715.11 | 1 | MST1L | 17089068 | rs7513616 | 1 | 17298496 | G | A | 0.43 | −0.06 | 0.02 | −0.03 | 6.88E-04 |
| ENSG00000140265.12 | 15 | ZSCAN29 | 43656796 | rs523156 | 15 | 43811843 | G | C | 0.53 | 0.08 | 0.03 | 0.04 | 7.75E-04 |
| ENSG00000014123.10 | 6 | UFL1 | 96986312 | rs11153023 | 6 | 96968525 | T | C | 0.15 | −0.12 | 0.03 | −0.07 | 8.19E-04 |
| ENSG00000237624.1 | 1 | OXCT2P1 | 39981395 | rs12028034 | 1 | 40039707 | A | G | 0.24 | 0.08 | 0.02 | 0.04 | 8.29E-04 |
| ENSG00000159363.19 | 1 | ATP13A2 | 17325438 | rs7513616 | 1 | 17298496 | G | A | 0.43 | 0.09 | 0.03 | 0.05 | 8.53E-04 |
| ENSG00000065717.15 | 19 | TLE2 | 3022635 | rs11150 | 19 | 2997897 | A | G | 0.17 | −0.17 | 0.05 | −0.09 | 9.46E-04 |
| ENSG00000268869.6 | 1 | ESPNP | 17030243 | rs7513616 | 1 | 17298496 | G | A | 0.43 | −0.12 | 0.04 | −0.06 | 1.36E-03 |
| **Anterior** | | | | | | | | | | | | | |
| ENSG00000272912.1 | 10 | AL356608.1 | 104674752 | rs10786719 | 10 | 104637992 | G | A | 0.41 | −0.17 | 0.04 | −0.09 | 4.98E-05 |
| ENSG00000148842.18 | 10 | CNNM2 | 104674015 | rs7897654 | 10 | 104662458 | C | T | 0.28 | 0.10 | 0.02 | 0.05 | 6.62E-05 |
| ENSG00000162669.16 | 1 | HFM1 | 91798368 | rs17713417 | 1 | 91848784 | T | C | 0.11 | 0.06 | 0.02 | 0.03 | 7.78E-05 |
| ENSG00000162461.8 | 1 | SLC25A34 | 16065320 | rs41393951 | 1 | 16053493 | A | G | 0.31 | −0.05 | 0.01 | −0.03 | 3.75E-04 |
| ENSG00000137760.15 | 11 | ALKBH8 | 107404960 | rs2037827 | 11 | 107408592 | C | T | 0.21 | −0.11 | 0.03 | −0.05 | 3.79E-04 |
| ENSG00000065060.17 | 6 | UHRF1BP1 | 34805354 | rs6906129 | 6 | 34801160 | C | T | 0.51 | −0.05 | 0.02 | −0.03 | 4.60E-04 |
| ENSG00000156052.11 | 9 | GNAQ | 80488870 | rs4582625 | 9 | 80520544 | C | T | 0.26 | −0.08 | 0.02 | −0.05 | 6.44E-04 |
| ENSG00000257354.2 | 12 | AC048341.1 | 63006262 | rs17731893 | 12 | 63013773 | A | G | 0.18 | 0.27 | 0.08 | 0.16 | 6.70E-04 |
| ENSG00000231305.4 | 3 | AC112484.1 | 128584923 | rs789217 | 3 | 128593201 | A | G | 0.26 | 0.04 | 0.01 | 0.02 | 7.64E-04 |
| ENSG00000164402.13 | 6 | IL20RA | 137343712 | rs9494644 | 6 | 137403294 | G | C | 0.31 | 0.21 | 0.06 | 0.12 | 7.80E-04 |
| **Posterior** | | | | | | | | | | | | | |
| ENSG00000138111.14 | 10 | MFSD13A | 104228977 | rs11593583 | 10 | 104228149 | G | A | 0.56 | −0.16 | 0.04 | −0.10 | 1.23E-04 |
| ENSG00000168386.18 | 3 | FILIP1L | 99691171 | rs6809988 | 3 | 99656615 | A | G | 0.22 | 0.13 | 0.03 | 0.07 | 2.75E-04 |
| ENSG00000213903.9 | 14 | LTB4R | 24783949 | rs11158632 | 14 | 24769663 | G | T | 0.22 | −0.23 | 0.06 | −0.13 | 4.01E-04 |
| ENSG00000148842.18 | 10 | CNNM2 | 104764015 | rs7897654 | 10 | 104662458 | C | T | 0.28 | 0.11 | 0.03 | 0.06 | 4.11E-04 |
| ENSG00000223959.8 | 16 | AFG3L1P | 90053782 | rs2270459 | 16 | 89979851 | A | C | 0.11 | −0.21 | 0.06 | −0.11 | 4.48E-04 |
| ENSG00000111615.14 | 12 | KRR1 | 75895030 | rs2070162 | 12 | 75900588 | G | A | 0.25 | −0.06 | 0.02 | −0.03 | 4.60E-04 |
| ENSG00000214043.8 | 12 | LINC02347 | 126940360 | rs17577161 | 12 | 126842742 | G | A | 0.34 | 0.06 | 0.02 | 0.04 | 5.97E-04 |
| ENSG00000255595.5 | 12 | AC007368.1 | 126797235 | rs17577161 | 12 | 126842742 | G | A | 0.34 | −0.07 | 0.02 | −0.04 | 6.18E-04 |
| ENSG00000258839.4 | 16 | MC1R | 89982954 | rs2270459 | 16 | 89979851 | A | C | 0.11 | 0.22 | 0.06 | 0.13 | 6.36E-04 |
| ENSG00000256310.1 | 12 | NDUFA5P6 | 127008983 | rs17577161 | 12 | 126842742 | G | A | 0.34 | 0.09 | 0.02 | 0.05 | 6.78E-04 |

*Significant functional genes at P value <8.4E-06. AF indicates allele 1 frequency; Allele1, effect allele (allele2 is another allele); BAD, brain arterial diameter; beta_BR_ss, effect size estimate correcting for the winner's curse by bootstrap resampling (BR_squared) method; eQTL, expression quantitative trait loci; GWAS, genome-wide association study; and SNV, single-nucleotide variant.
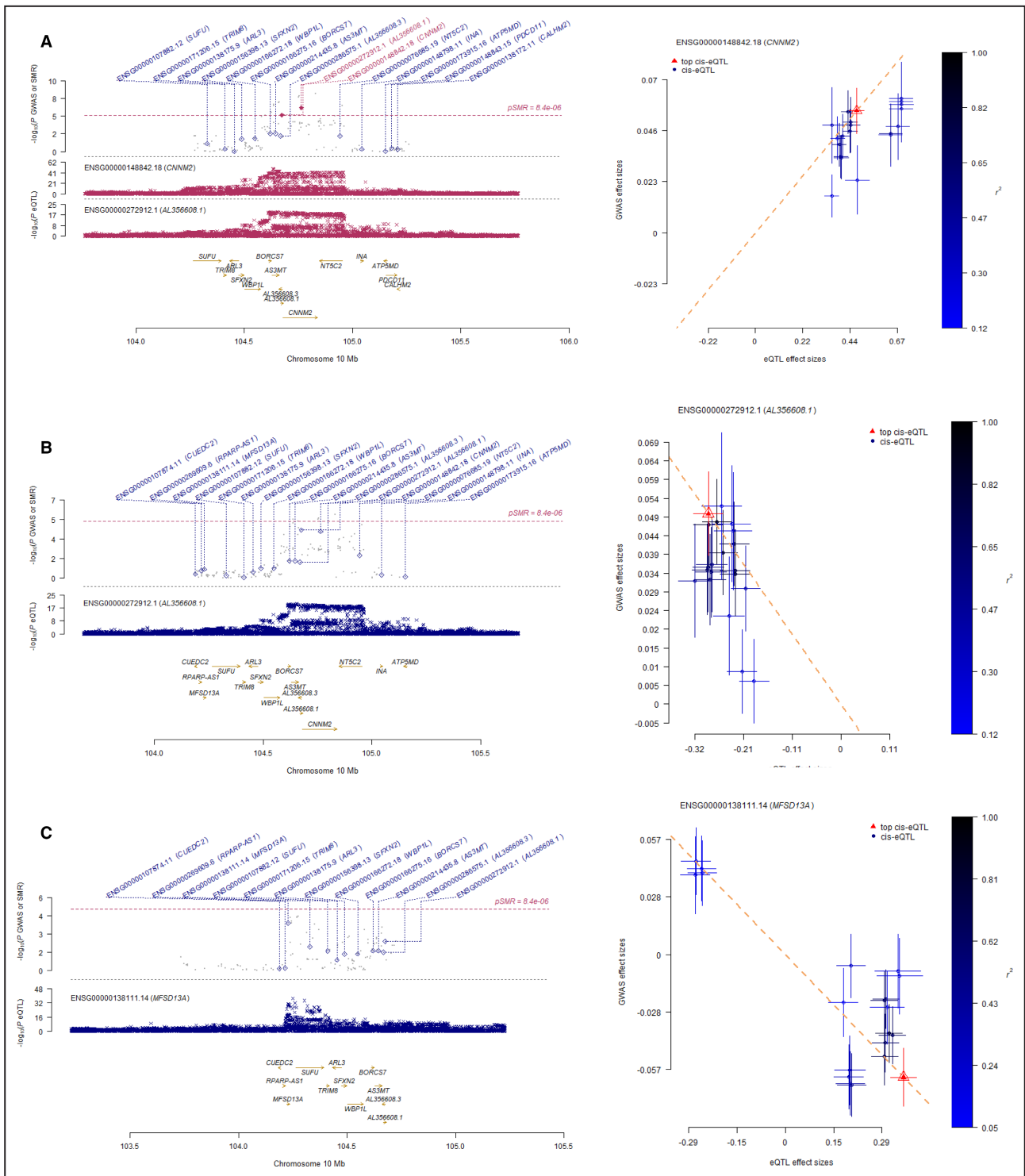
**Figure 3.** Locus plot and effect sizes plot of genome-wide association study (GWAS) and expression quantitative trait loci (eQTL) associations.
**A**, Global brain arterial diameter (BAD). **B**, Anterior BAD. **C**, Posterior BAD.

## Causal Pathway From BAD to AD, Stroke, and White Matter Hyperintensities Volume

To establish a causal pathway from BAD to AD, stroke, and white matter hyperintensities volume, we performed MR analysis (Tables S11 and S12). We did not observe any association of BAD with AD, stroke, or white matter hyperintensities volume.

## Pleiotropic Locus for Anterior and Posterior BAD

MTAG analysis used the fixed-effect meta-analysis estimates for anterior and posterior BAD. Since global BAD is the average of anterior and posterior BAD, the global estimate was excluded from multivariate analysis. No genomic inflation was observed in trans-ancestry analysis (Figure S9). MTAG results of joint analysis BAD did not show any genome-wide significant SNVs (Tables S13 and S14).

## DISCUSSION

This is the first study, to our knowledge, to examine the genetic determinants of BAD in an ancestrally diverse population, where we identified associations of novel genetic loci with BAD genetic architecture. Beyond mapping to the nearest genes, we also showed the biological impact of our findings using in silico functional analyses. Our results demonstrated that multiple genetic loci were coupled with gene expression information, which imply biologically relevant pathways.

We identified a novel BAD locus at 10q24.32 mapped to *CNNM2*. *CNNM2* encodes cyclin M2, which is a member of magnesium ($Mg^{2+}$) transporters. As an abundant intracellular divalent cation in the human body, $Mg^{2+}$ plays an important role in numerous biological processes such as the synthesis of RNA, DNA, and protein, and the production and storage of cellular energy.[46] *CNNM2* is involved in brain development, neurological functioning, and $Mg^{2+}$ homeostasis.[47] Heterozygous variants in the *CNNM2* gene can cause renal hypomagnesemia (HOMG6 [MIM 613882]), seizures, and intellectual disability (HOMGSMR1 [MIM 616418]).[48] In our study, variant rs7897654 was associated with decreased BAD ($\beta$=−0.06) and increased *CNNM2* expression ($\beta$=0.02) (Table 4). The variant rs7897654 colocalized with eQTL of *CNNM2*, confirming its functional relationship to this gene. Our study also identified a variant in *TCF25* associated at genome-wide significance with posterior BAD. *TCF25* is a member of the basic helix–loop–helix family of transcription factors that are important in embryonic development.[49] These 2 results suggest that the effects of these genetic variants on arterial size might be present early in life, but how aging interacts with these variants remains unknown.

The *NT5C2* encodes a phosphatase involved in cellular purine metabolism, which is associated with disorders characterized by psychiatric and psychomotor disturbances.[50,51] *NT5C2* has a high affinity for adenosine monophosphate and is involved in the extensive transcriptional programming that regulates cell maintenance, proliferation, migration, and differentiation during neurodevelopment.[52–55] *NT5C2* has also been shown to negatively regulate phosphorylation of the alpha subunit of 5′-adenosine monophosphate–activated protein kinase and protein translation.[56] Studies in the Chinese Han population report that *NT5C2* rs2148198 is associated with coronary heart disease susceptibility, and *NT5C2* rs11191580 is associated with schizophrenia and symptom severity.[57,58] In addition, a zebrafish study provides evidence that *NT5C2* and *CNNM2* are most likely the causal genes within a blood pressure locus at the 10q24.32.[59] Our trans-ancestry GWAS analysis identified a significant variant rs10748839, mapped on the 2KB upstream of *NT5C2*, which is a promoter variant that controls expression of *NT5C2*.[60]

The *AS3MT* gene, located in 10q24.32, encodes a cytosolic protein, which is a cysteine-rich enzyme that transfers a methyl group from S-adenosyl-L-methionine to trivalent arsenical.[61,62] *AS3MT* plays an important role in catalysis of biomethylation of arsenic in vivo and in vitro. *AS3MT* is mainly expressed in human adrenal glands, liver, heart, kidney, and brain.[63] In addition, *AS3MT* expression is highly expressed in adult human neurons and astrocytes during human stem cell differentiation toward neuronal fates and in brains of patients with schizophrenia compared with controls[64] and with attention-deficit or hyperactivity disorder.[65] Notably, *AS3MT* rs7085104 as a schizophrenia-associated risk SNV altered striatal dopamine synthesis capacity. Moreover, the *AS3MT-CNNM2-NT5C2* gene cluster region is involved in the cause and pathogenesis of schizophrenia and the 3 genes have been confirmed as schizophrenia susceptibility gene cluster.[66,67] Our study identified *AS3MT* rs10786721 variants with genome-wide significance in global BAD. In addition, *AS3MT* rs72841270 is a lead variant associated with global BAD in Hispanic-specific populations. Whether neuronal connectivity or network formation indirectly or directly impacts BADs is unclear but should be further studied.

Lysosomes play a critical role in maintenance of the integrity of neuronal function, and mutations in genes that contribute to lysosome formation, transport, and activity are associated with neurodegenerative disorders.[68,69] Recently, the multisubunit complex, BLOC-one-related complex (BORC), has been shown to be involved in positioning lysosomes within the cytoplasm, although the consequences of altered BORC function in adult animals have not been established.[70,71] A study in mice identifies *BORCS7* (*C10orf32*) as a central factor in axonal transport of lysosomes and a possible target for improving disease-related disturbances in this important function; additionally, the Q87X mutation in the *BORCS7* subunit results in motor deficits and dystrophic axonopathy in mice.[72] In our gene-based MAGMA analysis, the significant associations for global BAD included *AS3MT*, *C10orf32*, *CNNM2*,

and *NT5C2*; we suspect that this 4-gene cluster region may be involved with the cause and pathogenesis of BAD, but the underlying mechanism is not clear.

Arterial diameters are routinely used by clinicians to assess vascular health. Previous studies have demonstrated that individuals with the smallest or largest BADs exhibit a higher incidence of vascular outcomes (eg, stroke, myocardial infarction, vascular death), when compared with individuals with less extreme forms of arterial remodeling.[5] This suggests that BADs may be used as surrogates of systemic and cerebral vascular health and that a combination of genetic and environmental factors may contribute to the development of extreme pathological forms of arterial diameters. Based on our results, we anticipate that the association between these genetic variants and BADs will be consistent across populations, although the effect size might vary given the presence of common confounders such as vascular risk factors (eg, hypertension, diabetes, dyslipidemia, and smoking status) and environmental exposures. To gain a comprehensive understanding, it is important for future studies to examine potential interactions between vascular risk factors and the factors analyzed in this study to determine their influence on BADs. Our study did not uncover any significant associations between BAD and AD, stroke, or white matter hyperintensity volume per se. To improve our understanding of the role of BAD in pathogenesis and clinical outcome, further studies should explore the association of BAD with specific clinical or radiological outcome, such as severity of cognitive decline. In addition, a replication study should be conducted to validate the genetic effects found significant in this study. According to the finding from discovery study,[59,66,67] in order to achieve a statistical power of 80% at a significance level of $5 \times 10^{-8}$, a replication study would require a sample size of approximately 6000 participants.

Our study is the first to explore the risk variants of BAD in a large multi-ancestry GWAS. We detected novel SNVs located in genomic region 10q24.32, which are associated with BAD. However, it is important to acknowledge certain study limitations. Lack of replication analysis may limit the reliability across different data sets or independent samples. Also, due to the modest sample sizes of Asian, African, and Hispanic participants, the statistical power to detect ancestry-specific associations or functional associations in these ancestries were limited. Consequently, unbalanced representation of ancestral groups may limit the applicability of the study's finding to specific ancestral groups. Similarly, disentangling the effects of these variants on overall brain health versus AD-specific pathways is difficult without functional analyses of genes related to arterial diameters, but exploring such pathways may reveal novel vascular contribution to AD and related dementias. In addition, we lacked screening for connective tissue disorder and vascular abnormalities, and were unable to investigate whether the presence of such conditions could potentially have an influence on our findings.

## CONCLUSIONS

In summary, we identified a novel genome-wide significant locus for BAD, *CNNM2*, *NT5C2*, and *AS3MT*, in a large multi-ancestry population. Our study provides a potential biological mechanism for the association between 10q24.32 variation and BAD. Identifying genes associated with these loci and their function may help us to elucidate the mechanism by which BADs may influence cerebrovascular health.

## Disclosures

None.

## Supplemental Material

Tables S1–S14.
Figures S1–S9.

## REFERENCES

1. Gutierrez J, Rosoklija G, Murray J, Chon C, Elkind MSV, Goldman J, Honig LS, Dwork AJ, Morgello S, Marshall RS. A quantitative perspective to the study of brain arterial remodeling of donors with and without hiv in the Brain Arterial Remodeling Study (BARS). *Front Physiol*. 2014;5:56. doi: 10.3389/fphys.2014.00056

2. Gutierrez J, Sacco RL, Wright CB. Dolichoectasia-an evolving arterial disease. *Nat Rev Neurol*. 2011;7:41–50. doi: 10.1038/nrneurol.2010.181

3. Smoker WR, Corbett JJ, Gentry LR, Keyes WD, Price MJ, McKusker S. High-resolution computed tomography of the basilar artery: 2. Vertebrobasilar dolichoectasia: clinical-pathologic correlation and review. *AJNR Am J Neuroradiol*. 1986;7:61–72.

4. Gutierrez J, Bagci A, Gardener H, Rundek T, Ekind MSV, Alperin N, Sacco RL, Wright CB. Dolichoectasia diagnostic methods in a multi-ethnic, stroke-free cohort: results from the northern Manhattan study. *J Neuroimaging*. 2014;24:226–231. doi: 10.1111/j.1552-6569.2012.00781.x

5. Gutierrez J, Cheung K, Bagci A, Rundek T, Alperin N, Sacco RL, Wright CB, Elkind MSV. Brain arterial diameters as a risk factor for vascular events. *J Am Heart Assoc*. 2015;4:e002289. doi: 10.1161/JAHA.115.002289

6. Gutierrez J, Guzman V, Khasiyev F, Manly J, Schupf N, Andrews H, Mayeux R, Brickman AM. Brain arterial dilatation and the risk of Alzheimer's disease. *Alzheimers Dement*. 2019;15:666–674. doi: 10.1016/j.jalz.2018.12.018

7. Gutierrez J, Kulick E, Park Moon Y, Dong C, Cheung K, Ahmet B, Stern Y, Alperin N, Rundek T, Sacco RL, et al. Brain arterial diameters and cognitive performance: the northern Manhattan study. *J Int Neuropsychol Soc*. 2018;24:335–346. doi: 10.1017/S1355617717001175

8. Pasterkamp G, Schoneveld AH, van Wolferen W, Hillen B, Clarijs RJ, Haudenschild CC, Borst C. The impact of atherosclerotic arterial remodeling on percentage of luminal stenosis varies widely within the arterial system. A postmortem study. *Arterioscler Thromb Vasc Biol*. 1997;17:3057–3063. doi: 10.1161/01.ATV.17.11.3057

9. Xu WH, Li ML, Gao S, Ni J, Zhou LX, Yao M, Peng B, Feng F, Jin ZY, Cui LY. In vivo high-resolution mr imaging of symptomatic and asymptomatic middle cerebral artery atherosclerotic stenosis. *Atherosclerosis*. 2010;212:507–511. doi: 10.1016/j.atherosclerosis.2010.06.035

10. Groenink M, den Hartog AW, Franken R, Radonic T, de Waard V, Timmermans J, Scholte AJ, van den Berg MP, Spijkerboer AM, Marquering HA, et al. Losartan reduces aortic dilatation rate in adults with Marfan syndrome: a randomized controlled trial. *Eur Heart J*. 2013;34:3491–3500. doi: 10.1093/eurheartj/eht334

11. Morris SA, Orbach DB, Geva T, Singh MN, Gauvreau K, Lacro RV. Increased vertebral artery tortuosity index is associated with adverse outcomes in children and young adults with connective tissue disorders. *Circulation*. 2011;124:388–396. doi: 10.1161/CIRCULATIONAHA.110.990549

12. Naunheim MR, Walcott BP, Nahed BV, MacRae CA, Levinson JR, Ogilvy CS. Arterial tortuosity syndrome with multiple intracranial aneurysms: a case report. *Arch Neurol*. 2011;68:369–371. doi: 10.1001/archneurol.2011.29

13. Gutierrez J, DiTullio M, Cheung YK, Alperin N, Bagci A, L Sacco R, B Wright C, Elkind MSV, Rundek T. Brain arterial dilatation modifies the association between extracranial pulsatile hemodynamics and brain perivascular spaces: the Northern Manhattan Study. *Hypertens Res*. 2019;42:1019–1028. doi: 10.1038/s41440-019-0255-1

14. Wright JD, Folsom A, Coresh J, Sharrett AR, Couper D, Wagenknecht LE, Mosley TH, Ballantyne CM, Boerwinkle EA, Rosamond WD, et al. The ARIC (Atherosclerosis Risk in Communities) study. *J Am Coll Cardiol*. 2021;77:2939–2959. doi: 10.1016/j.jacc.2021.04.035

15. Knopman DS, Gottesman RF, Sharrett AR, Wruck LM, Windham BG, Coker L, Schneider AL, Hengrui S, Alonso A, Coresh J, et al. Mild cognitive impairment and dementia prevalence: the Atherosclerosis Risk in Communities Neurocognitive Study (ARIC-NCS). *Alzheimers Dement*. 2016;2:1–11. doi: 10.1016/j.dadm.2015.12.002

16. Manly JJ, Bell-McGinty S, Tang MX, Schupf N, Stern Y, Mayeux R. Implementing diagnostic criteria and estimating frequency of mild cognitive impairment in an urban community. *Arch Neurol*. 2005;62:1739–1746. doi: 10.1001/archneur.62.11.1739

17. Foong AW, Saw SM, Loo JL, Shen S, Loon SC, Rosman M, Aung T, Tan DT, Tai ES, Wong TY. Rationale and methodology for a population-based study of eye diseases in Malay people: the Singapore Malay Eye Study (SiMES). *Ophthalmic Epidemiol*. 2007;14:25–35. doi: 10.1080/09286580600878844

18. Lavanya R, Jeganathan VS, Zheng Y, Raju P, Cheung N, Tai ES, Wang JJ, Lamoureux E, Mitchell P, Young TL, et al. Methodology of the Singapore Indian Chinese Cohort (SICC) eye study: quantifying ethnic variations in the epidemiology of eye diseases in Asians. *Ophthalmic Epidemiol*. 2009;16:325–336. doi: 10.3109/09286580903144738

19. Wong TY, Chong EW, Wong WL, Rosman M, Aung T, Loo JL, Shen S, Loon SC, Tan DT, Tai ES, et al. Prevalence and causes of low vision and blindness in an urban Malay population: the Singapore Malay Eye Study. *Arch Ophthalmol*. 2008;126:1091–1099.

20. Zheng Y, Lavanya R, Wu R, Wong WL, Wang JJ, Mitchell P, Cheung N, Cajucom-Uy H, Lamoureux E, Aung T, et al. Prevalence and causes of visual impairment and blindness in an urban Indian population: the Singapore Indian Eye Study. *Ophthalmology*. 2011;118:1798–1804. doi: 10.1016/j.ophtha.2011.02.014

21. von Elm E, Altman DG, Egger M, Pocock SJ, Gotzsche PC, Vandenbroucke JP; STROBE Initiative. The Strengthening the Reporting of Observational Studies in Epidemiology (STROBE) statement: guidelines for reporting observational studies. *J Clin Epidemiol*. 2008;61:344–349. doi: 10.1016/j.jclinepi.2007.11.008

22. Suinesiaputra A, de Koning PJ, Zudilova-Seinstra E, Reiber JH, van der Geest RJ. Automated quantification of carotid artery stenosis on contrast-enhanced MRA data using a deformable vascular tube model. *Int J Cardiovasc Imaging*. 2012;28:1513–1524. doi: 10.1007/s10554-011-9988-x

23. Qiao Y, Guallar E, Suri FK, Liu L, Zhang Y, Anwar Z, Mirbagheri S, Xie YJ, Nezami N, Intrapiromkul J, et al. MR imaging measures of intracranial atherosclerosis in a population-based study. *Radiology*. 2016;280:860–868. doi: 10.1148/radiol.2016151124

24. Gutierrez J, Khasiyev F, Liu M, DeRosa JT, Tom SE, Rundek T, Cheung K, Wright CB, Sacco RL, Elkind MSV. Determinants and outcomes of asymptomatic intracranial atherosclerotic stenosis. *J Am Coll Cardiol*. 2021;78:562–571. doi: 10.1016/j.jacc.2021.05.041

25. Li Y, Willer CJ, Ding J, Scheet P, Abecasis GR. Mach: using sequence and genotype data to estimate haplotypes and unobserved genotypes. *Genet Epidemiol*. 2010;34:816–834. doi: 10.1002/gepi.20533

26. Das S, Forer L, Schonherr S, Sidore C, Locke AE, Kwong A, Vrieze SI, Chew EY, Levy S, McGue M, et al. Next-generation genotype imputation service and methods. *Nat Genet*. 2016;48:1284–1287. doi: 10.1038/ng.3656

27. Loh PR, Danecek P, Palamara PF, Fuchsberger C, Reshef YA, Finucane HK, Schoenherr S, Forer L, McCarthy S, Abecasis GR, et al. Reference-based phasing using the Haplotype Reference Consortium panel. *Nat Genet*. 2016;48:1443–1448. doi: 10.1038/ng.3679

28. Willer CJ, Li Y, Abecasis GR. METAL: fast and efficient meta-analysis of genomewide association scans. *Bioinformatics*. 2010;26:2190–2191. doi: 10.1093/bioinformatics/btq340

29. Mägi R, Horikoshi M, Sofer T, Mahajan A, Kitajima H, Franceschini N, McCarthy MI; Cogent-Kidney Consortium T2D-GENES Consortium, Morris AP. Trans-ethnic meta-regression of genome-wide association studies accounting for ancestry increases power for discovery and improves fine-mapping resolution. *Hum Mol Genet*. 2017;26:3639–3650. doi: 10.1093/hmg/ddx280

30. Turley P, Walters RK, Maghzian O, Okbay A, Lee JJ, Fontana MA, Nguyen-Viet TA, Wedow R, Zacher M, Furlotte NA, et al. Multi-trait analysis of genome-wide association summary statistics using MTAG. *Nat Genet*. 2018;50:229–237. doi: 10.1038/s41588-017-0009-4

31. Forde A, Hemani G, Ferguson J. Review and further developments in statistical corrections for Winner's Curse in genetic association studies. *PLoS Genet*. 2023;19:e1010546. doi: 10.1371/journal.pgen.1010546

32. de Leeuw CA, Mooij JM, Heskes T, Posthuma D. MAGMA: generalized gene-set analysis of GWAS data. *PLoS Comput Biol*. 2015;11:e1004219. doi: 10.1371/journal.pcbi.1004219

33. Watanabe K, Taskesen E, van Bochoven A, Posthuma D. Functional mapping and annotation of genetic associations with FUMA. *Nat Commun*. 2017;8:1826. doi: 10.1038/s41467-017-01261-5

34. GTEx Consortium. Human genomics. The Genotype-Tissue Expression (GTEx) pilot analysis: multitissue gene regulation in humans. *Science*. 2015;348:648–660. doi: 10.1126/science.1262110

35. Liberzon A, Birger C, Thorvaldsdottir H, Ghandi M, Mesirov JP, Tamayo P. The Molecular Signatures Database (MSigDB) hallmark gene set collection. *Cell Syst*. 2015;1:417–425. doi: 10.1016/j.cels.2015.12.004

36. Slenter DN, Kutmon M, Hanspers K, Riutta A, Windsor J, Nunes N, Melius J, Cirillo E, Coort SL, Digles D, et al. Wikipathways: a multifaceted pathway database bridging metabolomics to other omics research. *Nucleic Acids Res*. 2018;46:D661–D667. doi: 10.1093/nar/gkx1064

37. Buniello A, MacArthur JAL, Cerezo M, Harris LW, Hayhurst J, Malangone C, McMahon A, Morales J, Mountjoy E, Sollis E, et al. The NHGRI-EBI GWAS catalog of published genome-wide association studies, targeted arrays and summary statistics 2019. *Nucleic Acids Res*. 2019;47:D1005–D1012. doi: 10.1093/nar/gky1120

38. Kircher M, Witten DM, Jain P, O'Roak BJ, Cooper GM, Shendure J. A general framework for estimating the relative pathogenicity of human genetic variants. *Nat Genet*. 2014;46:310–315. doi: 10.1038/ng.2892

39. Zhu Z, Zhang F, Hu H, Bakshi A, Robinson MR, Powell JE, Montgomery GW, Goddard ME, Wray NR, Visscher PM, et al. Integration of summary data from GWAS and eQTL studies predicts complex trait gene targets. *Nat Genet*. 2016;48:481–487. doi: 10.1038/ng.3538

40. Qi T, Wu Y, Zeng J, Zhang F, Xue A, Jiang L, Zhu Z, Kemper K, Yengo L, Zheng Z, et al. Identifying gene targets for brain-related traits using transcriptomic and methylomic data from blood. *Nat Commun*. 2018;9:2282. doi: 10.1038/s41467-018-04558-1

41. Bellenguez C, Küçükali F, Jansen IE, Kleineidam L, Moreno-Grau S, Amin N, Naj AC, Campos-Martin R, Grenier-Boley B, Andrade V, et al. New insights into the genetic etiology of Alzheimer's disease and related dementias. *Nat Genet*. 2022;54:412–436. doi: 10.1038/s41588-022-01024-z

42. Malik R, Rannikmäe K, Traylor M, Georgakis MK, Sargurupremraj M, Markus HS, Hopewell JC, Debette S, Sudlow CLM, Dichgans M. Genome-wide meta-analysis identifies 3 novel loci associated with stroke. *Ann Neurol*. 2018;84:934–939. doi: 10.1002/ana.25369

43. Elliott LT, Sharp K, Alfaro-Almagro F, Shi S, Miller KL, Douaud G, Marchini J, Smith SM. Genome-wide association studies of brain imaging phenotypes in UK Biobank. *Nature*. 2018;562:210–216. doi: 10.1038/s41586-018-0571-7

44. Davies NM, Hill WD, Anderson EL, Sanderson E, Deary IJ, Davey SG. Multivariable two-sample Mendelian randomization estimates of the effects of intelligence and education on health. *eLife*. 2019;8:8. doi: 10.7554/eLife.43990

45. Hemani G, Zheng J, Elsworth B, Wade KH, Haberland V, Baird D, Laurin C, Burgess S, Bowden J, Langdon R, et al. The MR-ase platform supports systematic causal inference across the human phenome. *eLife*. 2018;7:7. doi: 10.7554/eLife.34408

46. Volpe SL. Magnesium in disease prevention and overall health. *Adv Nutr*. 2013;4:378s–383s. doi: 10.3945/an.112.003483

47. Accogli A, Scala M, Calcagno A, Napoli F, Di Iorgi N, Arrigo S, Mancardi MM, Prato G, Pisciotta L, Nagel M, et al. CNNM2 homozygous mutations cause severe refractory hypomagnesemia, epileptic encephalopathy and brain malformations. *Eur J Med Genet*. 2019;62:198–203. doi: 10.1016/j.ejmg.2018.07.014

48. Stuiver M, Lainez S, Will C, Terryn S, Günzel D, Debaix H, Sommer K, Kopplin K, Thumfart J, Kampik NB, et al. CNNM2, encoding a basolateral protein required for renal Mg2+ handling, is mutated in dominant hypomagnesemia. *Am J Hum Genet*. 2011;88:333–343. doi: 10.1016/j.ajhg.2011.02.005

49. Steen H, Lindholm D. Nuclear localized protein-1 (Nulp1) increases cell death of human osteosarcoma cells and binds the X-linked inhibitor of apoptosis protein. *Biochem Biophys Res Commun*. 2008;366:432–437. doi: 10.1016/j.bbrc.2007.11.146

50. Duarte RRR, Bachtel ND, Cotel MC, Lee SH, Selvackadunco S, Watson IA, Hovsepian GA, Troakes C, Breen GD, Nixon DF, et al. The psychiatric risk gene NT5C2 regulates adenosine monophosphate-activated protein kinase signaling and protein translation in human neural progenitor cells. *Biol Psychiatry*. 2019;86:120–130. doi: 10.1016/j.biopsych.2019.03.977

51. Singgih EL, van der Voet M, Schimmel-Naber M, Brinkmann EL, Schenck A, Franke B. Investigating cytosolic 5′-nucleotidase ii family genes as candidates for neuropsychiatric disorders in drosophila (114/150 chr). *Transl Psychiatry*. 2021;11:55. doi: 10.1038/s41398-020-01149-x

52. Itoh R. Enzymatic properties and physiological roles of cytosolic 5′-nucleotidase ii. *Curr Med Chem*. 2013;20:4260–4284. doi: 10.2174/0929867311320340006

53. Hoffman GE, Schrode N, Flaherty E, Brennand KJ. New considerations for hiPSC-based models of neuropsychiatric disorders. *Mol Psychiatry*. 2019;24:49–66. doi: 10.1038/s41380-018-0029-1

54. Tang Y, Illes P. Regulation of adult neural progenitor cell functions by purinergic signaling. *Glia*. 2017;65:213–230. doi: 10.1002/glia.23056

55. Tornroth-Horsefield S, Neutze R. Opening and closing the metabolite gate. *Proc Natl Acad Sci U S A*. 2008;105:19565–19566. doi: 10.1073/pnas.0810654106

56. Kulkarni SS, Karlsson HK, Szekeres F, Chibalin AV, Krook A, Zierath JR. Suppression of 5′-nucleotidase enzymes promotes AMP-activated protein kinase (AMPK) phosphorylation and metabolism in human and mouse skeletal muscle. *J Biol Chem*. 2011;286:34567–34574. doi: 10.1074/jbc.M111.268292

57. Chen X, Zhang Z, Wang X, Chen Y, Wang C. NT5C2 gene polymorphisms and the risk of coronary heart disease. *Public Health Genomics*. 2020;23:90–99. doi: 10.1159/000507714

58. Li Z, Jiang J, Long J, Ling W, Huang G, Guo X, Su L. The rs11191580 variant of the *NT5C2* gene is associated with schizophrenia and symptom severity in a South Chinese Han population: evidence from GWAS. *Braz J Psychiatry*. 2017;39:104–109. doi: 10.1590/1516-4446-2016-1958

59. Vishnolia KK, Hoene C, Tarhbalouti K, Revenstorff J, Aherrahrou Z, Erdmann J. Studies in zebrafish demonstrate that CNNM2 and NT5C2 are most likely the causal genes at the blood pressure-associated locus on human chromosome 10q24.32. *Front Cardiovasc Med*. 2020;7:135. doi: 10.3389/fcvm.2020.00135

60. Mitra AK, Crews KR, Pounds S, Cao X, Feldberg T, Ghodke Y, Gandhi V, Plunkett W, Dolan ME, Hartford C, et al. Genetic variants in cytosolic 5′-nucleotidase ii are associated with its expression and cytarabine sensitivity in HapMap cell lines and in patients with acute myeloid leukemia. *J Pharmacol Exp Ther*. 2011;339:9–23. doi: 10.1124/jpet.111.182873

61. Lin S, Shi Q, Nix FB, Styblo M, Beck MA, Herbin-Davis KM, Hall LL, Simeonsson JB, Thomas DJ. A novel S-adenosyl-L-methionine:arsenic(III) methyltransferase from rat liver cytosol. *J Biol Chem*. 2002;277:10795–10803. doi: 10.1074/jbc.M110246200

62. Liu WS, Wang XY, Lu X, Zhang YM, Ye XM, Li JM, Zhao QL, Wu ZQ, Zhou J, Hai X. Polymorphisms in arsenic (+3 oxidation state) methyltransferase (AS3MT) predict the occurrence of hyperleukocytosis and arsenic metabolism in APL patients treated with As(2)O(3). *Arch Toxicol*. 2020;94:1203–1213. doi: 10.1007/s00204-020-02686-6

63. Su AI, Cooke MP, Ching KA, Hakak Y, Walker JR, Wiltshire T, Orth AP, Vega RG, Sapinoso LM, Moqrich A, et al. Large-scale analysis of the human and mouse transcriptomes. *Proc Natl Acad Sci U S A*. 2002;99:4465–4470. doi: 10.1073/pnas.012025199

64. Li M, Jaffe AE, Straub RE, Tao R, Shin JH, Wang Y, Chen Q, Li C, Jia Y, Ohi K, et al. A human-specific AS3MT isoform and BORCS7 are molecular risk factors in the 10q24.32 schizophrenia-associated locus. *Nat Med*. 2016;22:649–656. doi: 10.1038/nm.4096

65. Zhao W, Zhang Q, Chen X, Li Y, Li X, Du B, Deng X, Ji F, Wang C, Xiang YT, et al. The VNTR of the *AS3MT* gene is associated with brain activations during a memory span task and their training-induced plasticity. *Psychol Med*. 2021;51:1927–1932. doi: 10.1017/S0033291720000720

66. Duarte RRR, Troakes C, Nolan M, Srivastava DP, Murray RM, Bray NJ. Genome-wide significant schizophrenia risk variation on chromosome

10q24 is associated with altered cis-regulation of BORCS7, AS3MT, and NT5C2 in the human brain. *Am J Med Genet B Neuropsychiatr Genet*. 2016;171:806–814. doi: 10.1002/ajmg.b.32445

67. Guan F, Zhang T, Li L, Fu D, Lin H, Chen G, Chen T. Two-stage replication of previous genome-wide association studies of AS3MT-CNNM2-NT5C2 gene cluster region in a large schizophrenia case-control sample from Han Chinese population. *Schizophr Res*. 2016;176:125–130. doi: 10.1016/j.schres.2016.07.004

68. Navone F, Genevini P, Borgese N. Autophagy and neurodegeneration: insights from a cultured cell model of als. *Cell*. 2015;4:354–386. doi: 10.3390/cells4030354

69. Menzies FM, Fleming A, Caricasole A, Bento CF, Andrews SP, Ashkenazi A, Füllgrabe J, Jackson A, Jimenez Sanchez M, Karabiyik C, et al. Autophagy and neurodegeneration: pathogenic mechanisms and therapeutic opportunities. *Neuron*. 2017;93:1015–1034. doi: 10.1016/j.neuron.2017.01.022

70. Pu J, Schindler C, Jia R, Jarnik M, Backlund P, Bonifacino JS. BORC, a multisubunit complex that regulates lysosome positioning. *Dev Cell*. 2015;33:176–188. doi: 10.1016/j.devcel.2015.02.011

71. Jia R, Guardia CM, Pu J, Chen Y, Bonifacino JS. BORC coordinates encounter and fusion of lysosomes with autophagosomes. *Autophagy*. 2017;13:1648–1663. doi: 10.1080/15548627.2017.1343768

72. Snouwaert JN, Church RJ, Jania L, Nguyen M, Wheeler ML, Saintsing A, Mieczkowski P, Manuel de Villena FP, Armao D, Moy SS, et al. A mutation in the Borcs7 subunit of the lysosome regulatory BORC complex results in motor deficits and dystrophic axonopathy in mice. *Cell Rep*. 2018;24:1254–1265. doi: 10.1016/j.celrep.2018.06.118